# Electronic Supplementary Information

## Efficient and complete dehydrogenation of hydrazine borane over a CoPt catalyst

Haochong Wu,[a] Qilu Yao*[,a] Chenxi Hu,[a] Jianjun Long,[a] Yuanlan Zhou,[a] Zhang-Hui Lu*[,a]

[a]*Institute of Advanced Materials (IAM), Key Laboratory of Energy Catalysis and Conversion of Nanchang, College of Chemistry and Chemical Engineering, Jiangxi Normal University, Nanchang 330022, China*

[b]*School of Mathematics and Statistics, Jiangxi Normal University, Nanchang 330022, China*

*E-mail: yaoqilu@jxnu.edu.cn (Q. L. Yao); luzh@jxnu.edu.cn (Z.-H. Lu)

# Table of Contents

## Experimental Section

**Chemicals and Materials:** All chemicals used in this work were purchased from commercial suppliers and used without further purification. Sodium borohydride ($NaBH_4$, Sinopharm Chemical Reagent Co., Ltd, 96%), cobalt chloride hexahydrate ($CoCl_2 \cdot 6H_2O$, Aladdin, AR), cerium (III) nitrate hexahydrate ($Ce(NO_3)_3 \cdot 6H_2O$, 99.5%), potassium tetra-chloroplatinate (II) ($K_2PtCl_4$, J&K Chemical, 99.95%), sodium hydroxide (NaOH, Tianjin ZhiYuan Reagent Co., Ltd, 96.0%), hydrazine hemisulfate salt ($N_2H_4 \cdot 1/2H_2SO_4$, Sigma-Aldrich, ⩾98%), 1,4-Dioxane($(C_2H_4)_2O_2$, Tianjin ZhiYuan Reagent Co., Ltd, ⩾99.5%), and ethanol ($CH_3CH_2OH$, Tianjin ZhiYuan Reagent Co., Ltd, ⩾99.7%) were used as received. Ultrapure water (R=18 MΩ cm) was obtained by reversed osmosis followed by ion exchanged and filtration.

**Syntheses of hydrazine borane:** Hydrazine borane (HB, $N_2H_4BH_3$) was synthesized according to previous work.[S1,S2] Generally, 21.42 g of hydrazine hexahydrate and 10.0 g of sodium borohydride are added to 160 mL of anhydrous 1,4-dioxane under stirring, and stirred at 303 K for 48 h under argon atmosphere. Then, the obtained turbid solution is centrifuged to obtain a clear solution. Then dry the filtrate at 333 K for 2 h through a rotary evaporator. The obtained crude $N_2H_4BH_3$ was further washed with n-pentene, and finally dried in vacuum at 313 K for 24 h to obtain white solid $N_2H_4BH_3$.

**Synthesis of $CeO_2$ nanorod:** $CeO_2$ nanorods were prepared by hydrothermal method.[S3] Generally, 1.75 g $Ce(NO_3)_3$ (4 mmol) was dissolved in 5 mL of deionized water, while 14.55 g NaOH (360 mmol) was dissolved in 55 mL of deionized water. Then $Ce(NO_3)_3$

solution was slowly dropped into NaOH solution and stirred at room temperature for 30 min. Then the mixed solution was transferred into a Teflon liner (100 mL) and keep at 100 ℃ for 24 h. After cooling to room temperature, the faint yellow precipitate was collected by centrifugation, washed several times with deionized water and ethanol, and then dried in the oven at 80 ℃ for 12 h. Finally, the $CeO_2$ nanorods were obtained by further annealed at 550 ℃ for 2 h in air.

**Syntheses of CoPt/$CeO_2$ catalysts:** The synthesis of CoPt/$CeO_2$ was synthesized by a facile, green, and low-cost wet-chemical reduction method at 298 K. Typically, for the synthesis of $Co_9Pt_1/CeO_2$, 10 mg of activated $CeO_2$ nanorods was dispersed in 5 mL deionized water. Then 10.9 mg of $CoCl_2 \cdot 6H_2O$ (0.045 mmol) and 2.1 mg of $K_2PtCl_4$ (0.005 mmol) were added to the $CeO_2$ suspension and sonicated for 30 min at 298 K. After that, quickly add 50 mg of $NaBH_4$ to the above mixture and stir vigorously. Finally, the black product of $Co_9Pt_1/CeO_2$ was obtained until the bubble generation ceased and directly used for the catalytic reaction without separation. The synthesis of $Co_xPt_{10-x}/CeO_2$ with different Co molar contents (x = 0, 1, 3, 5, 7, 9and 10) was carried out following an analogous process. For comparison, the $Co_9M_1/CeO_2$ (M = Pt, Ir, Rh, Ru and Pd) and $M_9Pt_1/CeO_2$ (M = Co, Ni, Cu and Fe) were also prepared by the same method as $Co_9Pt_1/CeO_2$.

**Characterization:** Powder X-ray diffraction (XRD) measurements were performed on a Rigaku Rint 2200 X-ray diffractometer with Cu Kα source (40 KV, 200mA). The

microscopic morphologies and size were investigated by scanning electron microscopy (SEM, SU-8020) and transmission electron microscopy (TEM, JEM-2100) coupled with an energy dispersive X-ray (EDX) detector for elemental analysis. X-ray photoelectron spectroscopy (XPS) measurements were obtained on an Thermo Scientific ESCALAB Xi+ with an Al Kα X-ray source after Ar sputtering for 15 s. The chemical compositions of the catalysts were determined by an inductively coupled plasma (ICP) spectrophotometer (Agilent 730 ) after each sample was completely dissolved in a mixture of $HNO_3$/HCl (1/3 ratio). The surface area and pore size distribution were obtained on a micromeritics BELSORP-mini Ⅱ at 77 K adopting the Brunauer-Emmett-Teller (BET) method. $CO_2$-temperature programmed desorption ($CO_2$-TPD) experiments were carried out on a Micromeritics AutoChem II 2920 automated system, equipped with a thermal conductivity detector. The gas compositions were determined by using a gas chromatograph (GC-9790 Ⅱ) with a thermal conductivity detector (TCD) and a TDX-01 chromatographic column (oven temperature: 333 K, detector temperature 393K).

**Catalytic activity measurement:** Typically, the catalytic reactions were carried out in a 50 mL round-bottom flask containing uniformly dispersed CoPt/$CeO_2$ catalyst suspension solution and NaOH (2.0 M, 5 mL). The reaction flask was then taken on a heated stirrer with the temperature set to 323 K. Subsequently, $N_2H_4BH_3$ (1 mmol) was added to the reactor, and the reaction started under vigorous stirring. Before measuring the gas produced by the dehydrogenation reaction, the gas was passed through a trap

containing a solution of HCl (1.0 M). The molar number of Co and Pt for all the catalytic reactions was kept at 0.05 mmol.

**Calculation method:** The $H_2$ selectivity for $N_2H_4BH_3$ (α) dehydrogenation is calculated by the following reaction formulas (Eqs. (S1-S2):

$$N_2H_4BH_3 + 3H_2O \rightarrow B(OH)_3 + (3 + 2\alpha)\ H_2 + (2\alpha+1)/3\ N_2 + 4(1-\alpha)/3NH_3 \quad (S1)$$

$$\alpha = \frac{3\lambda - 10}{8}\left[\lambda = \frac{n(H_2 + N_2)}{n(N_2H_4BH_3)}\left(\frac{10}{3} \leq \lambda \leq 6\right)\right] \quad (S2)$$

The turn over frequency (*TOF*) reported in this work is an apparent *TOF* value based on the number of metal (Co + Pt) atoms in catalysts, which is calculated from the equation as follow:

$$TOF = \frac{n(H_2)}{n(metal) \times t} \quad (S3)$$

Where $nH_2$ is the mole number of generated $H_2$, $n$metal is the total mole number of Co and Pt in catalyst, and $t$ is the completed reaction time.

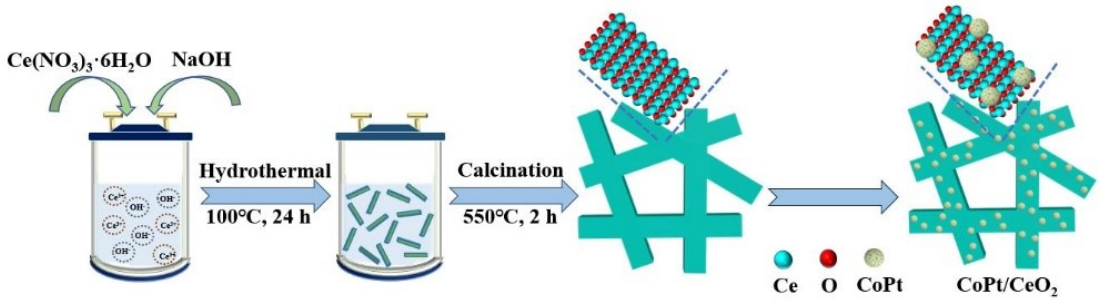


**Fig. S1** Schematic illustration of the preparation of $CoPt/CeO_2$.

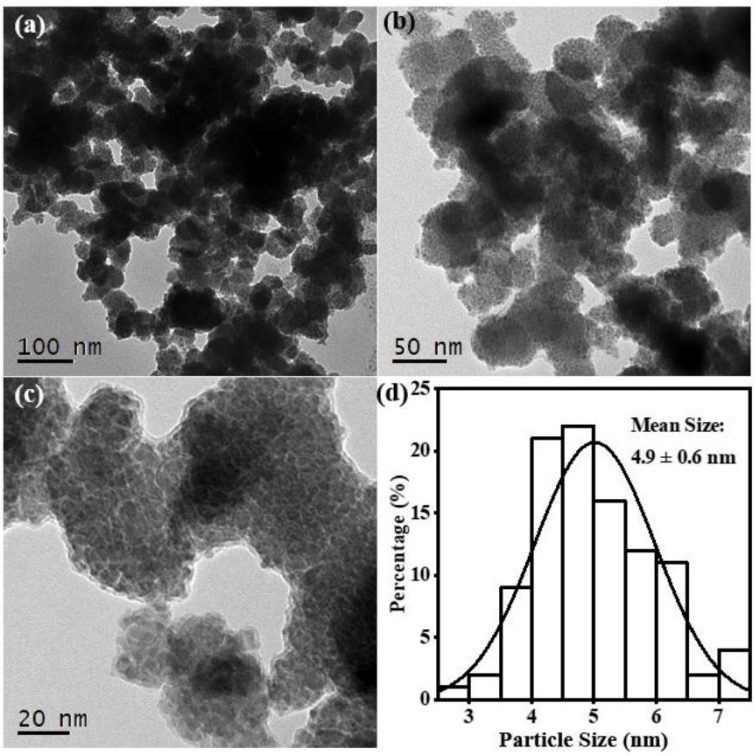


**Fig. S2** (a-c) TEM images and (d) particle size distribution of $Co_9Pt_1$ NPs.

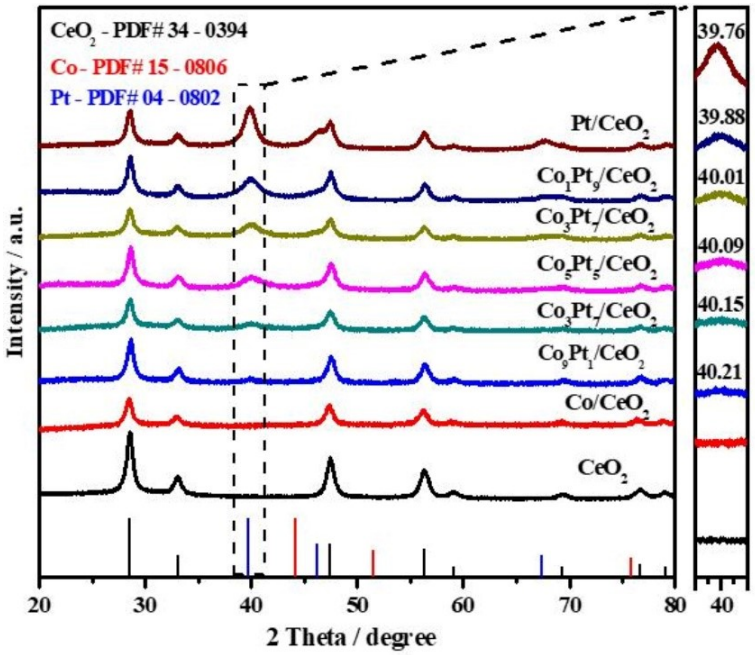


**Fig. S3** XRD patterns of $CoPt/CeO_2$ with different molar ratios of Co and Pt.

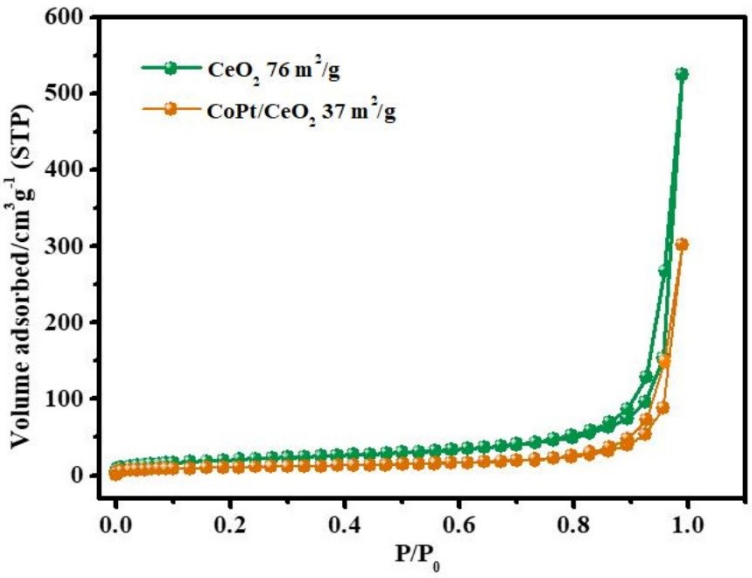


**Fig. S4** Nitrogen adsorption-desorption isotherms of $CeO_2$ and $Co_9Pt_1/CeO_2$.

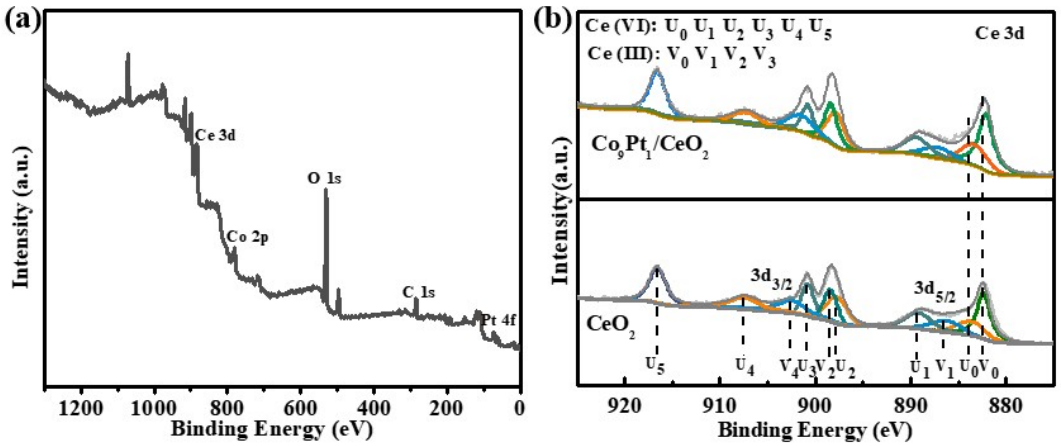


**Fig. S5** (a) Survey XPS spectrum of $Co_9Pt_1/CeO_2$ and (b) Ce 3d XPS spectra of the synthesized samples.

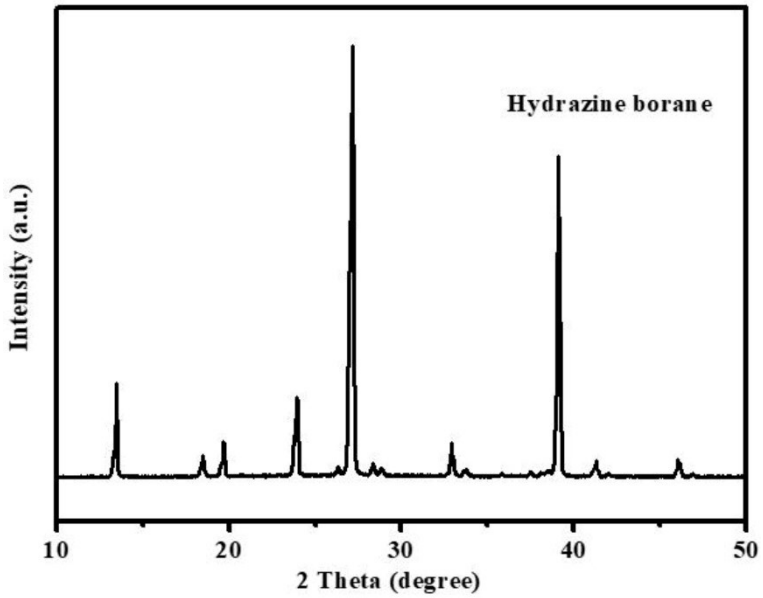


**Fig. S6** XRD pattern of $N_2H_4BH_3$.

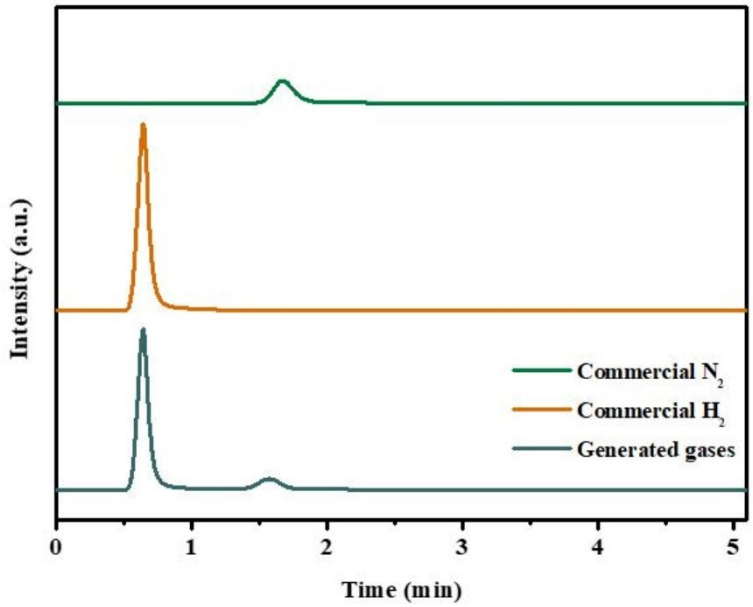


**Fig. S7** GC spectra using TCD for the commercial $H_2$, commercial $N_2$, and released gases from the decomposition of $N_2H_4BH_3$ over $Co_9Pt_1/CeO_2$.

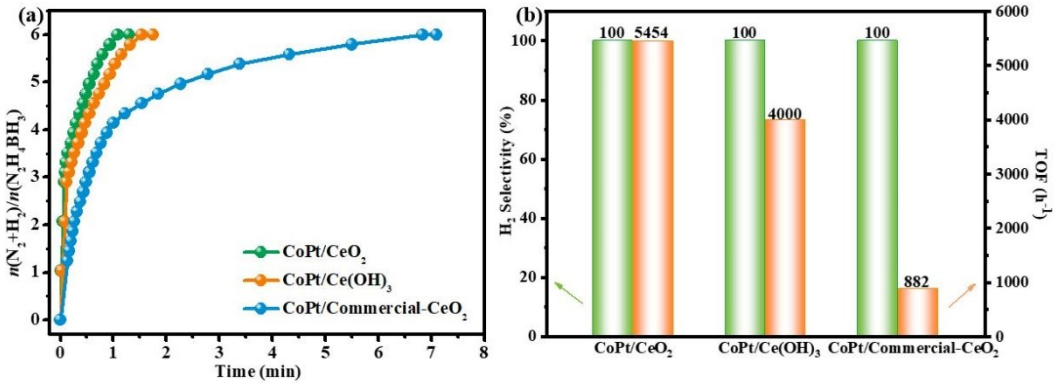


**Fig. S8** (a) Time course plots for hydrogen evolution from aqueous $N_2H_4BH_3$ solution (0.2 M, 5 mL) over CoPt/$CeO_2$, CoPt/$Ce(OH)_3$ and CoPt/Commercial-$CeO_2$ in the presence of NaOH (2.0 M) at 323 K ($n$metal/$nN_2H_4BH_3$ = 0.05). (b) The corresponding $H_2$ selectivity and TOF values.

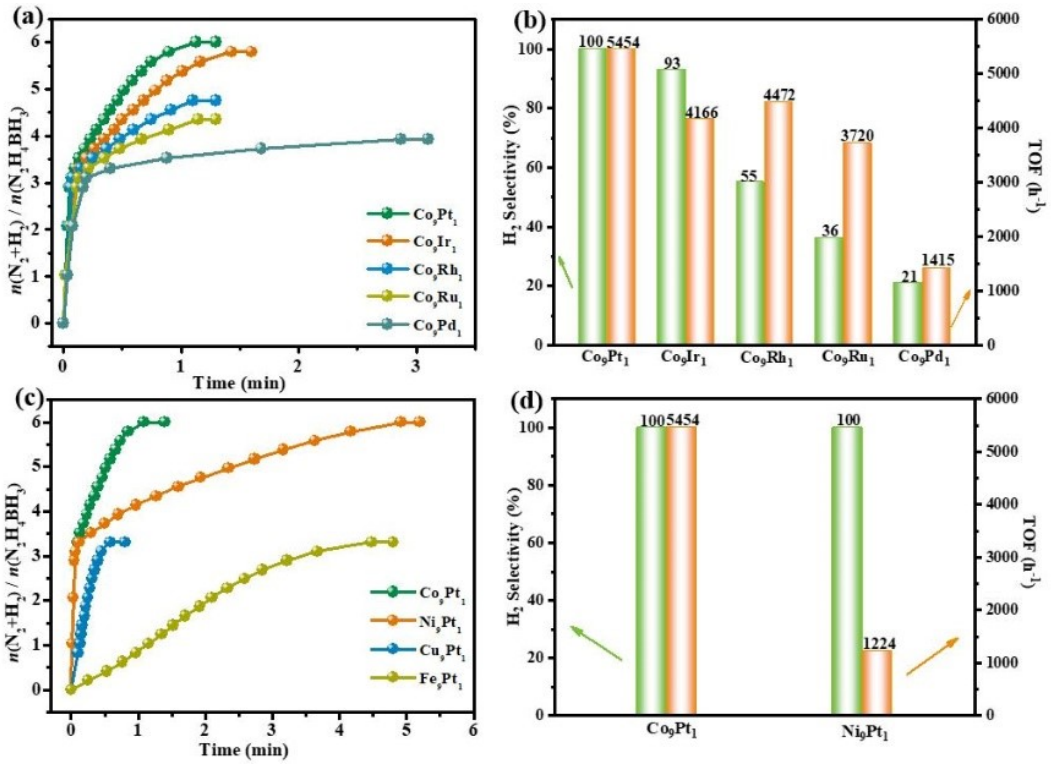


**Fig. S9** Time course plots and the corresponding $H_2$ selectivity and TOF values for hydrogen evolution from aqueous $N_2H_4BH_3$ solution (0.2 M, 5 mL) over (a,b) $Co_9M_1/CeO_2$ (M = Pt, Ir, Rh, Ru and Pd) and (c,d) $M_9Pt_1/CeO_2$ (M = Co, Ni, Cu and Fe) in the presence of NaOH (2.0 M) at 323 K ($n$metal/$nN_2H_4BH_3$ = 0.05).

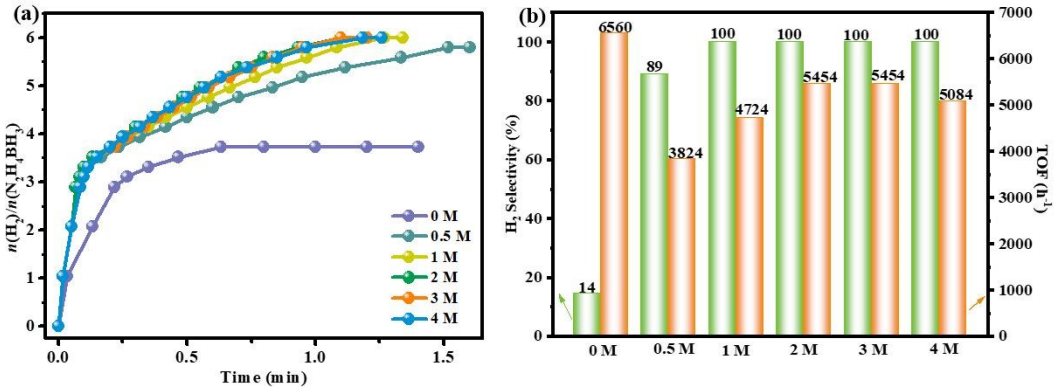


**Fig. S10** (a) Time course plots for hydrogen evolution from aqueous $N_2H_4BH_3$ solution (0.2 M, 5 mL) over $Co_9Pt_1/CeO_2$ with different concentrations of NaOH at 323 K ($n$CoPt/$n N_2H_4BH_3$ = 0.05). (b) The corresponding $H_2$ selectivity and TOF values.

NaOH can act as a promoter to strengthen the catalytic performance for $N_2H_4BH_3$ dehydrogenation.[S4] Thus, the catalytic activity of as-synthesized $Co_9Pt_1/CeO_2$ for $N_2H_4BH_3$ dehydrogenation was tested under different concentrations of NaOH. As shown in the Fig. S10, just less than 3.7 equiv. of gas is generated in the absence of NaOH, indicating the incomplete dehydrogenation of $N_2H_4BH_3$. It should be noticed that the catalytic activity and hydrogen selectivity of $Co_9Pt_1/CeO_2$ are both evidently enhanced by the introduction of NaOH. Specially, with the introduction of NaOH increased to 2.0 M, the $Co_9Pt_1/CeO_2$ catalyst exhibits the optimal catalytic efficiency. The possible reasons for the promotion are as follows: firstly, $OH^-$ ions can improve the rate determining deprotonation step ($N_2H_4 \rightarrow N_2H_3^* + H^*$), and secondly, the generation process of $NH_3$ can be prevented in the alkaline condition.

**Table S1** The catalysts composition determined by inductively coupled plasma atomic emission spectroscopic (ICP-OES).

| Catalysts | Co (wt%) | Pt (wt%) | Co/Pt theoretical molar ratio | Co/Pt actual molar ratio |
|---|---|---|---|---|
| $Co_9Pt_1/CeO_2$ | 19.06 | 6.58 | 9.0:1.0 | 9.1:0.9 |
| $Co_7Pt_3/CeO_2$ | 13.45 | 19.84 | 7.0:3.0 | 6.9:3.1 |
| $Co_5Pt_5/CeO_2$ | 8.06 | 25.96 | 5.0:5.0 | 5.1:4.9 |
| $Co_3Pt_7/CeO_2$ | 4.99 | 30.99 | 3.0:7.0 | 3.5:6.5 |
| $Co_1Pt_9/CeO_2$ | 1.64 | 41.19 | 1.0:9.0 | 1.2:8.8 |

**Table S2** Activity comparison of different catalysts for $N_2H_4BH_3$ dehydrogenation.

| Catalysts | T (K) | NaOH (M) | $H_2$ selectivity (%) | TOF ($h^{-1}$) | $E_{a1}(BH_3)$ (kJ $mol^{-1}$) | $E_{a2}(N_2H_4)$ (kJ $mol^{-1}$) | Ref. |
|---|---|---|---|---|---|---|---|
| **$CoPt/CeO_2$** | **323** | **2.0** | **100** | **5454** | **20.9** | **33.5** | **This Work** |
| NiPt-$MoO_x$/$NH_2$-N-rGO | 323 | 1.5 | 100 | 4412 | 36.1 | 46.2 | S5 |
| Ni@Ir/OMS-2 | 323 | 5.0 | 100 | 3300 | -- | -- | S6 |
| NiPt-$CeO_x$/MIL-101 | 323 | 1.0 | 100 | 2951 | 10.5 | 43.9 | S7 |
| NiPt/DT-$Ti_3C_2Tx$ | 323 | 1.0 | 100 | 2027 | 32.4 | 64.3 | S8 |
| NiPt/MIL-101 | 323 | 0.5 | 100 | 1515 | 18.6 | 44.6 | S9 |
| NiIr/$La_2O_2CO_3$ | 323 | 1.5 | 100 | 1250 | 16.3 | 57.7 | S10 |
| RhNi/MIL-101 | 323 | 0.5 | 100 | 1200 | 17.5 | 47.1 | S11 |
| NiPt-$Cr_2O_3$ | 323 | 0.5 | 100 | 1200 | 30.6 | 64.4 | S12 |
| RhNi@$CeO_x$/rGO | 323 | 0.5 | 100 | 667 | 18.6 | 56.9 | S4 |
| NiPd-$MoO_x$ | 323 | 2.0 | 100 | 405 | 49.7 | 72.6 | S13 |
| NiPt/graphene | 323 | 0.5 | 100 | 240 | -- | -- | S14 |
| NiPt-$CeO_2$ | 323 | 0.5 | 90 | 234 | -- | -- | S15 |
| RhNi NPs | 323 | 2.0 | 93 | 90 | -- | -- | S16 |
| Ni@(RhNi-alloy)/$Al_2O_3$ | 323 | -- | 90 | 72 | -- | -- | S17 |
| NiFePd/MIL-101 | 323 | 2.0 | 100 | 60 | 30.3 | 58.1 | S18 |
| NiPt NPs | 323 | -- | 93 | 18 | -- | -- | S19 |

## References


S1 Q. L. Zhu, D. C. Zhong, U. B. Demirci and Q. Xu, *ACS Catal.*, 2014, **4**, 4261-4268.

S2 J. J. Long, Q. L. Yao, X. L. Zhang, H. C. Wu and Z. H. Lu, *Appl. Catal. B Environ.*, 2023, **302**, 121989.

S3 Y. C. Wei, Y. L. Zhang, P. Zhang, J. Xiong, X. L. Mei, Q. Yu, Z. Zhao and J. Liu, *Environ. Sci. Technol*., 2020, **54**, 2002-2011.

S4 Z. J. Zhang, Z. H. Lu, H. L. Tan, X. S. Chen and Q. L. Yao, *J. Mater. Chem. A*, 2015, **3**, 23520-23529.

S5 X. Kang, J. X. Yao, Y. X. Duan, Z. Y. Chen, J. M. Yan and Q. Jiang, *J. Mater. Chem. A*, 2021, **9**, 26704-26708.

S6 M. Yurderi, T. Top, A. Bulut, G. S. Kanberoglu and M. Kaya, M. Zahmakiran, *Inorg. Chem*., 2020, **59**, 9728-9738.

S7 Y. X. Bai, Y. B. Liu, H. N. Shang, S. J. Li and J. S. Liang, *New J. Chem*., 2022, **46**, 13971-13980.

S8 F. Guo, H. T. Zou, Q. L. Yao, B. H and Z. H. Lu, *Renew Energy*, 2020, **155**, 1293-1301.

S9 Z. J. Zhang, S. L. Zhang, Q. L. Yao, X. S. Chen and Z. H. Lu, *Inorg. Chem*., 2017, **56**, 11938-11945.

S10 X. L. Hong, Q. L. Yao, M. L. Huang, H. X. Du and Z. H. Lu, *Inorg. Chem*. *Front*., 2019, **6**, 2271-2278.

S11 Z. J. Zhang, S. L. Zhang, Q. L. Yao, F. Guo, M. H. Zhu and Z. H. Lu, *Inorg. Chem. Front*., 2018, **5**, 370-377.

S12 J. M. Chen, Z. H. Lu, Q. L. Yao, G. Feng and Y. Luo, *J. Mater. Chem. A*, 2018, **6**, 20746-20752.

S13 Q. L. Yao, K. K. Yang, W. D. Nie, Y. X. Li and Z. H. Lu, *Renew. Energy*, 2020, **147**, 2024-2031.

S14 Z. J. Zhang, Z. H. Lu and X. S. Chen, *ACS Sustain. Chem. Eng*., 2015, **3**, 1255-1261.

S15 Z. J. Zhang, Y. Q. Wang, X. S. Chen and Z. H. Lu, *J. Power Sources*, 2015, **291**,14-19.

S16 D. C. Zhong, K. Aranishi, A. K. Singh, U. B. Demircib and Q. Xu, *Chem. Commun*., 2012, **48**, 11945-11947.

S17 C. M. Li, Y. B. Dou, J. Liu, Y. D. Chen, S. He, M. Wei, D. G. Evans and X. Duan, *Chem. Commun*., 2013, **49**, 9992-9994.

S18 K. Yang, K. K. Yang, S. L. Zhang, Y. Luo, Q. L. Yao and Z. H. Lu, *J. Alloy Compd*., 2018, **732**, 363-371.

S19 J. Hannauer, O. Akdim, U. B. Demirci, C. Geantet, J. M. Herrmann, P. Miele and Q. Xu, *Energy Environ. Sci*., 2011, **4**, 3355-3358.